*TNO report*
FEL-96-A073

# The ORFEO measurement campaign

TNO Physics and Electronics Laboratory

Oude Waalsdorperweg 63
PO Box 96864
2509 JG The Hague
The Netherlands

Phone +31 70 374 00 00
Fax +31 70 328 09 61

Date
August 1996

Author(s)
R. van der Heiden
J. de Vries



Classification

| | | |
|---|---|---|
| Classified by | : | W. Pelt |
| Classification date | : | 25 July 1996 |

| | | |
|---|---|---|
| Title | : | Ongerubriceerd |
| Managementuittreksel | : | Ongerubriceerd |
| Abstract | : | Ongerubriceerd |
| Report text | : | Ongerubriceerd |



| | | |
|---|---|---|
| Copy no | : | 7 |
| No of copies | : | 29 |
| No of pages | : | 37 (excl RDP & distribution list) |
| No of appendices | : | - |

All information which is classified according to Dutch regulations shall be treated by the recipient in the same way as classified information of corresponding value in his own country. No part of this information will be disclosed to any party.

The classification designation Ongerubriceerd is equivalent to Unclassified, Stg. Confidentieel is equivalent to Confidential and Stg. Geheim is equivalent to Secret.



The TNO Physics and Electronics Laboratory is part of TNO Defence Research which further consists of:

TNO Prins Maurits Laboratory
TNO Human Factors Research Institute

Netherlands Organization for Applied Scientific Research (TNO)

# Managementuittreksel

| | | |
|---|---|---|
| Titel | : | The ORFEO measurement campaign |
| Auteur(s) | : | Drs. R. van der Heiden, J. de Vries |
| Datum | : | augustus 1996 |
| Opdrachtnr. | : | A94KM673 |
| IWP-nr. | : | 760.1 |
| Rapportnr. | : | FEL-96-A073 |

In de laatste 50 jaar is de radar een zeer waardevol instrument gebleken voor het detecteren en volgen van vliegtuigen. Deze mogelijkheden laten echter een cruciale vraag onbeantwoord: *wat* hebben we nu gedetecteerd? Dit probleem, het herkennen van objecten met een radar, vormt de grondslag voor het onderzoek naar niet-coöperatieve doelclassificatie met radar (NCTR).

Op dit moment spitst het NCTR-onderzoek op TNO-FEL zich toe op de classificatie van afstandsprofielen: ééndimensionale radarafbeeldingen van vliegtuigen. Voor de identificatie van een onbekend object, echter, moeten we een bestand aanleggen van beelden waarvan we de herkomst kennen.

Dit rapport beschrijft de meetcampagne ORFEO (Opbouw van een Rangeprofiel bestand met de FELSTAR ten behoeve van het Onderzoek naar NCTR), die is uitgevoerd om een bestand te verwerven van afstandsprofielen van civiele vliegtuigen.

Een toekomstig classificatiesysteem dat werkt op basis van de ORFEO-afstandsprofielen kan altijd getest worden aangezien voortdurend civiele vliegtuigen in de buurt van TNO-FEL aanwezig zijn. Een tweede voordeel is dat geometrische modellen van vele civiele vliegtuigen te koop zijn in tegenstelling tot militaire vliegtuigen. Op TNO-FEL is software ontwikkeld om afstandsprofielen te voorspellen op basis van deze modellen. Gebruik makend van de ORFEO-meetcampagne kunnen deze technieken voor het gebruik in NCTR gevalideerd worden.

Deze meetcampagne is succesvol verlopen: er zijn ruim 30.000 afstandsprofielen gemeten van in totaal 17 verschillende vliegtuigen.

# Contents

# List of abbreviations

| | |
|---|---|
| HRR | High Range Resolution |
| NCTR | Non-Cooperative Target Recognition |
| FELSTAR | FEL S-Band Target Aquisition Radar |
| ORFEO | Opbouw van een Rangeprofiel bestand met de FElstar ten behoeve van het Onderzoek naar NCTR (range profile acquisition with the FELSTAR radar for NCTR research) |
| RAP | Recognised Air Picture |
| RRM | Rotational Range Migration |
| STC | SHAPE Technical Centre |
| PRI | Pulse Repetition Interval |
| AWACS | Airborne Warning And Control System |
| RCS | Radar Cross Section |

# 1 Introduction

Today's aircraft identification techniques are based on the cooperation of a target. The virtue of Non-Cooperative Target Recognition (NCTR) is that recognition can be obtained without the aircraft's active participation.

Simple and rapidly measurable aircraft signatures are range profiles. These are essentially one-dimensional "images", where the aircraft's radar scatterers are projected onto the line of sight.

At TNO-FEL, a target database of civil aircraft was gained using the FELSTAR S-Band radar. The measurement campaign, named ORFEO ("Opbouw van een Rangeprofiel bestand met de FElstar ten behoeve van het Onderzoek naar NCTR", that is, "range profile acquisition with the FELSTAR radar for NCTR research"), provided over 30,000 range profiles from 17 different civil aircraft of opportunity.

This report documents the measurement campaign. Its organisation is as follows: we will start with the objectives and motivation for carrying out the campaign. Then the instrumentation, i.e., the FELSTAR and the Recognised Air Picture, are described. Chapter 4 provides information on the air traffic near TNO-FEL. The succeeding chapter describes the waveform choice and its properties. The measurements itself and the used processing steps are found in chapters 6 and 7, respectively. The latter chapter also shows several results. Concluding remarks are made in the final chapter 8.

# 2 Motivation and Objectives

In the ORFEO measurement campaign, we intended to acquire a database of radar range profiles for research on Non-Cooperative Target Recognition (NCTR) by Radar. The targets were civil aircraft of opportunity. This database is of importance for the following reasons:

- The measurements will complement the currently available database of military aircraft.
- A future range profile classification method, trained with the ORFEO data, can easily be evaluated as in the vicinity of the FELSTAR civil aircraft are always present.
- Wireframe models of many civil aircraft are commercially available (company: Viewpoint Datalabs, Utah, US) in contrast to military aircraft. At TNO-FEL, software is developed to predict radar range profiles using these wireframe models [1]. In the near future a validation of the models and the prediction techniques will be performed using the ORFEO range profile measurements.

# 3 Instrumentation

## 3.1 The FELSTAR radar

FELSTAR is a radar system at TNO-FEL, designed and built to conduct radar experiments. The FELSTAR system is a fully transputer controlled radar and consists of the following subsystems:

### Antenna

- Parabolic reflector with a diameter of 4.5 m.
- Illumination by a monopulse cluster providing one sum channel and two difference channels (azimuth and elevation).
- Sum pattern is a pencil beam with a half-power beamwidth not larger than 1.2 degrees over the tuning bandwidth of the system.
- Antenna gain of the sum beam on the beam axis is not less than 39 dB; the sidelobes near the main beam are at least 31 dB down.
- Steering to any azimuth position over an elevation extent from -5 to 85 degrees ('software' limit). The antenna can be steered with a velocity of 30 degrees/s in azimuth and 15 degrees/s in elevation; the corresponding accelerations are 10 and 5 degrees/$s^2$.
- Vertical polarisation.

### Transmitter

- Transmission frequency can be selected over a bandwidth from 3000 to 3600 MHz on a grid of 0.1 MHz.
- Peak power of 10 kW. The pulse repetition interval is to be selected in steps of 0.1 $\mu s$ from 100 $\mu s$ to 1000 $\mu s$ - for the ORFEO measurements, a pulse repetition interval of 420 $\mu s$ was applied.
- Pulse lengths are available from 100 ns, restricted to combinations of pulse repetition frequency and pulse length with a maximum average transmitted power of 250 W. The maximum duty-cycle is 2.4%.
- The coherence will be retained over a pulse train; phase deviation will be less than 1 degree.

### Receiver

Monopulse processing in 3 reception channels over selected radar range.

- Receiver sum-, azimuth- and elevation channel.

- Quick-look Doppler processing.
- 3-pulse MTI canceler over total radar range.
- Tracking gate processing over total radar range.
- Output available in I and Q at 10 Msamples/s in 8 bits - this rate corresponds to a range resolution of 15 m.

**Data registration**

The system is provided with a real-time data buffer of 96 MBytes. Data output from the sum channel is stored in pulse compressed form. The time gate can be selected to be anything from a range cell up to a complete pulse interval. After completion of a run the buffer contents are transferred to a hard disk file server together with the relevant system parameters.

**User interface**

The user gives instructions to the system on a personal computer that is connected to the FELSTAR by a transputer link. The corresponding program is written in C. The program calls subprograms from a library of macro's which cover sub-tasks like the search of a specified volume, selection of a detected target based on user-specified conditions, tracking of a selected target, recording of a target in track *et cetera.* For quick view and analysis, relevant information about the system status is supplied on the PC screen and about the received radar echoes and target characteristics on a colour display.

## 3.2 The Recognised Air Picture

The Herwijnen Air Traffic Control radar provides the azimuth and range from aircraft above Dutch airspace. The secondary radar interrogates the aircraft, thereby providing the target height. Aircraft flightplans (containing the target type) are associated with these coordinates. In a cooperation project between STC and TNO-FEL (contract number A92KM772) this data has been made available on a so-called *Recognised Air Picture* or *RAP*.

For the user, it shows in real time on a computer screen a map of the Netherlands and the aircraft that are currently present in Dutch airspace. If for a particular aircraft a flightplan is available, more information can be displayed. For the ORFEO measurements the aircraft coordinates and the aircraft type are of interest.

The type is given in a four-digit string. Different series of the same aircraft may have the same name, e.g. the aircraft B73S denotes both the 300 and 500 series of the Boeing 737. For the use of range profiles in target classification this should always be kept in mind: profiles from (slightly) different aircraft belong to the same class.

# 4 Air traffic

At TNO-FEL we have the possibility to measure many different aircraft as Schiphol Airport is less than 27 km away. Both small jets for continental flights and large airliners for intercontinental flights can be observed. We limited ourselves to civil aircraft of opportunity in the corridors and aircraft that are leaving or entering the corridors. Where possible we avoided measurements during curves to prevent large roll angles. As a consequence, aircraft were not measured that were very close to landing or that had just taken off.

During several days in June 1994 it was monitored which aircraft were present in Dutch airspace. They are listed in the following table in the order of decreasing probability of occurrence. In the second column a unique target number is given - this number is used in the data base. A histogram is shown in figure 4.1. It demonstrates that the twenty selected aircraft types (from a total of the 220 civil aircraft that occurred at least once) are responsible for 72% of all occurrences.

| *Code* | *Target no* | *Manufacturer* | *Model* |
|---|---|---|---|
| B73S | 115 | Boeing | 737-300/500 series |
| B737 | 113 | Boeing | 737-100/200 series |
| B73F | 114 | Boeing | 737-400 |
| FK50 | 458 | Fokker | 50 |
| FK10 | 454 | Fokker | 100 |
| SF34 | 964 | Saab | SF340 |
| MD80 | 686 | McDonnel-Douglas | MD80-/81/82/83/87/88 |
| B747 | 116 | Boeing | 747-100/200/300 series |
| EA32 | 401 | Airbus | 320 |
| B757 | 120 | Boeing | 757, all series |
| EA31 | 400 | Airbus | A310 |
| B767 | 121 | Boeing | 767, all series |
| FK28 | 457 | Fokker | Fellowship F28 |
| DC9 | 344 | McDonnel-Douglas | DC-9-20/30/40/50 |
| E120 | 378 | Embraer | Brasilia EMB-120/HH/RT |
| B74F | 117 | Boeing | 747-400 |
| FK27 | 456 | Fokker | 27 |
| BA46 | 126 | British Aerospace | BAe 146-100/200/300 |
| L101 | 628 | Lockheed | Tri-Star, all series |
| DC10 | 334 | McDonnel-Douglas | DC-10, all series |

Three peaks of increased air traffic be identified during the day. A first wave of incoming traffic starts at approximately 7:30 am and ends at 10:00 am. Outbound traffic is due from approximately 12:30 until 14:00 pm. An

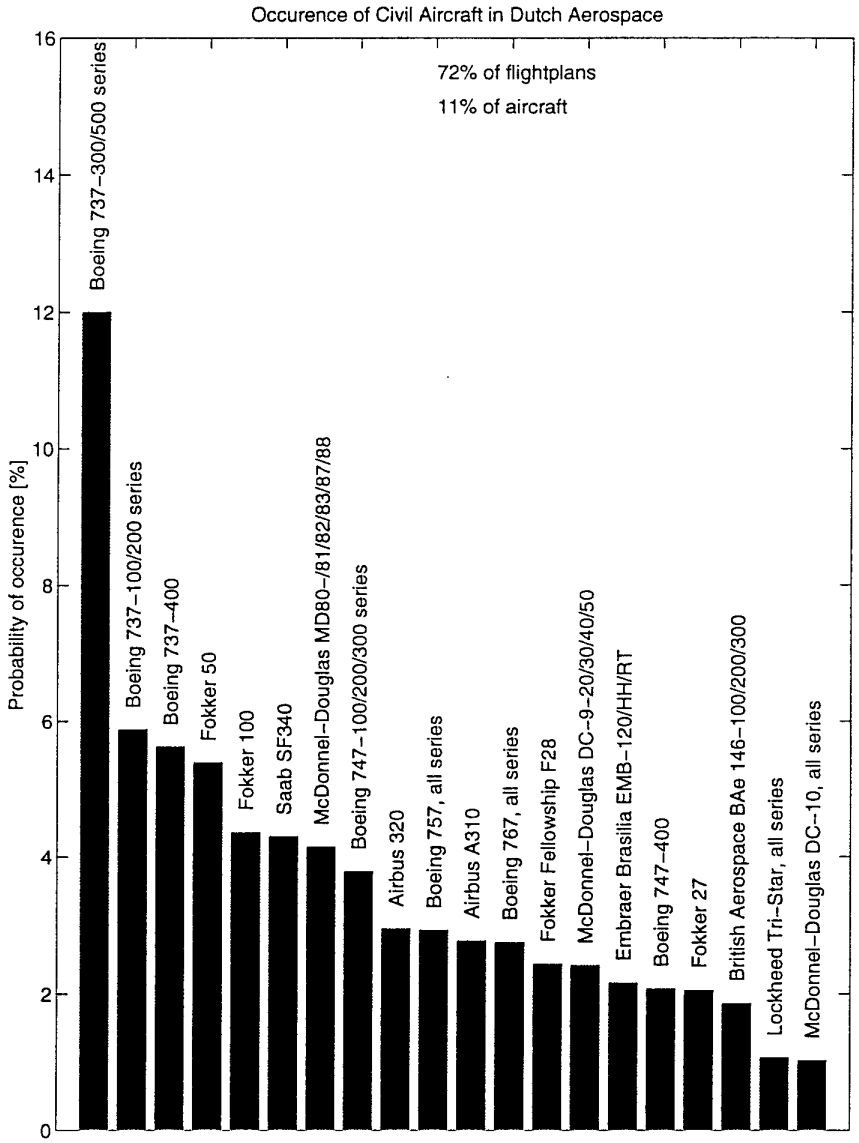


*Figure 4.1*: Occurrence histogram of aircraft types in Dutch air space during four days in June 1994.

increase in both inbound and outbound traffic is to be expected between 17:00 h and 20:00 h, pm. This information served as a guideline for the planning of the measurements.

# 5 Waveform choice

For the waveform we have chosen:

| | | |
|---|---|---|
| Waveform type | : | velocity tolerant |
| First frequency | : | 3073.8 MHz |
| Frequency step | : | 1.4 MHz |
| Number of pulses | : | 324 |
| Minimum pulse repetition interval | : | 420 $\mu$s |
| Pulse width | : | 1.5 $\mu$s |
| Range gate resolution | : | 75 m |
| Range gate | : | 1500 m (20 samples) |
| Sampling resolution | : | 8 bits |

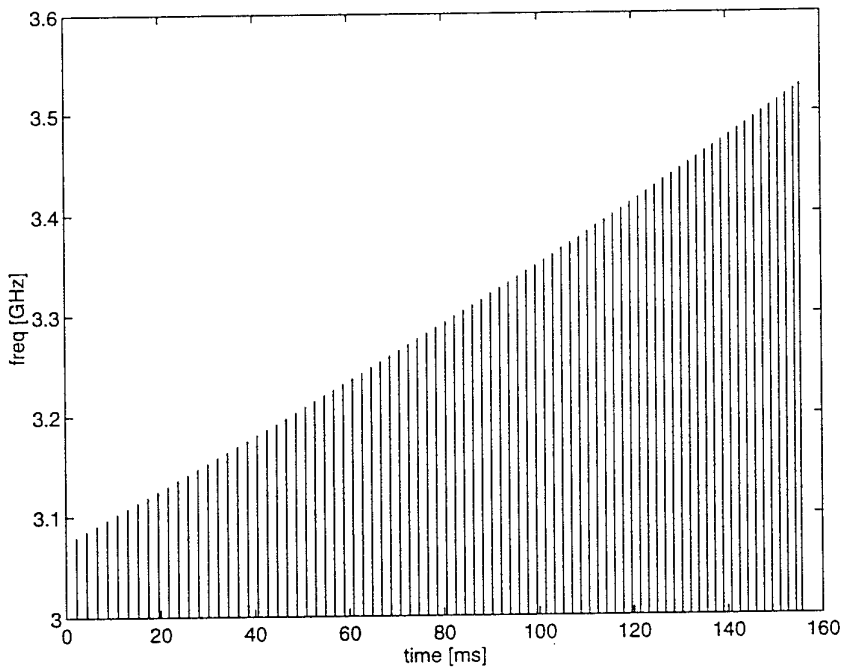


*Figure 5.1*: Waveform used at the ORFEO measurement campaign. Only the pulses $1, 5, 9, \ldots, 321$ and 324 are shown. Although it is hardly observable, the pulse-repetition interval decreases with frequency.

The properties of this waveform are:

1. *Unambiguous range window*

This window must be larger than the dimension of the largest aircraft that can be expected. For the chosen waveform this window equals 107 m, considerably larger than the optical dimensions of the largest civil aircraft (approximately 60 m).

2. *Range resolution*

   The nominal range resolution of the range profile equals 32 cm. In the data processing of chapter 7, we use a Hamming window. This increases the resolution to approximately 42 cm.

3. *Maximum distance*

   De maximum distance at which aircraft can be measured is 60 km (corresponding to a round-trip time of $400\mu s$). Before a pulse can be emitted, a *silent* or *dead* period of $20\mu s$ is required by the radar hardware. Hence we find a minimum pulse repetition frequency of $420\mu s$.

4. *Waveform duration*

   The total waveform duration is 156.0 ms.

5. *Number of pulses*

   The number of pulses can be decomposed in factors 2 and 3: $324 = 2^2 3^4$. If one does not alter this using e.g. zeropadding or *Burg extension* [2] this factorisation can be exploited to speed up the Fourier analysis.

6. *Rotational Range Migration*

   During the emission of a waveform the aircraft rotates with respect to the line of sight to the radar.

   From the rotation rate and the aircraft size we may compute the differential displacement between the most left hand side scatterer on the aircraft and the most right hand side scatterer. If this displacement is larger than the range resolution, then we have the undesired effect of *rotational range migration* (RRM).

   Suppose the outermost scatterers are separated by 60 m (worst case). Then the angle over which RRM occurs equals 0.32 degrees. The rotation of the aircraft may not be as high that this amount is exceeded. The maximum allowable rotation rate is therefore 2.0 deg/s.

   As a practical worst case, take a tangential aircraft crossing with a velocity $v = 250$ m/s and at a range $R = 10$ km. Then for the rotation rate we find 1.4 deg/s which is well below the limit.

7. *Aircraft translation*

The special waveform type, used for the first time in FELSTAR measurements, ensures that no velocity compensation is needed afterwards [3, 4]. Also, this waveform is fairly insensitive to acceleration: if $|a| \lessapprox \frac{\sqrt{3}\lambda}{T^2} = 7.1\mathrm{m/s}^2$ acceleration compensation is not necessary [3]. If, again, we consider the tangential passing of an aircraft with velocity $v$ and at a range $R$ then the maximum acceleration is $v^2/R$. Taking $R = 10$ km and $v = 250$ m/s it follows that the maximum acceleration equals 6.3 m/s$^2$, which can be tolerated.

8. *JEM line suppression*

   Another positive side effect using the velocity tolerant waveform instead of the common linear waveform (equal time-steps between pulses) can be mentioned. Jet Engine Modulation (JEM) lines are caused by the reflections on the aircraft engines and can be used to identify aircraft. For measuring range profiles with a linear waveform the JEM lines are, however, a nuisance as they cause disturbances throughout the range profile. In the velocity tolerant waveform the time delays are not equal, but vary smoothly. The result is that the JEM lines are effectively decorrelated [4].

9. *Pulse width*

   The pulse width is three times as large as the Range Gate Resolution. It means that the target will be seen in three of the twenty samples.

10. *Measurement time*

    The maximum capacity of the databuffer equals $24 \times 10^6$ samples. Per pulse 20 samples are stored. The net measurement time of a full data buffer is therefore just below 10 minutes.

# 6 The measurements

## 6.1 Procedures

During the measurements, one person operates the FELSTAR and the other the Recognised Air Picture. The latter searches for an aircraft on the RAP screen that

- has a range of less than 60 km from the FELSTAR;
- has a flightplan not older than several minutes;
- belongs to one of the twenty most frequently encountered aircraft (see table page 10);
- has an elevation higher than one degree;
- has an azimuth not in the range 220° to 360° (this is due to obscuration by obstacles on the roof of the TNO-FEL building);
- is not manouvering due to a recent take-off or due to an intended landing.

If a suitable target is found, the RAP-operator waits for a new update and communicates the coordinates to the radar operator. He inserts them into the FELSTAR control program. Then, the radar searches for a box around these coordinates with sizes 15°, 3° and 30 km for azimuth, elevation and range, respectively. We experienced that in most cases the target was found in a single scan through the box. If detection failed, new coordinates were inserted or a new target was selected.

After detection, the antenna gain needs to be adjusted manually. This is to avoid saturation if the gain is too high or a low signal-to-noise ratio if the gain is too low. In both cases, the track can be lost.

The FELSTAR control program displays the coordinates of the target in track. This information is cross-checked with a new RAP update so as to be sure that the correct target is in track. If this is indeed the case and if the target is not performing a curve, registration is started.

For several measurements, the flightplan was apparently incorrectly associated with the target as, during measurement, the flightplan was not updated. The target type was therefore suspicious. We did not assign a class to these measurements but gave them the label '????'.

The dates, times, aircraft types and possible remarks were written down on log-sheets.

In total, 77 measurements were made from seventeen different aircraft (apart from the targets with suspicious type). Several measurements were very short (several tens of profiles) to perform a system test, e.g. measurements 3, 17 and 18. The following two tables list the measurements. The columns are:

1. *Date*
2. *File*

   Each file contains one contiguous sequence of fully processed range profiles from the same target. The format is a MATLAB data file. The file is self-explanatory: if it is loaded in MATLAB using, e.g.,
   `>> load 0036.mat`
   then displaying the variable `VARIABLES` with
   `>> VARIABLES`
   shows the description of the file contents.
3. *Meas.*

   Measurement number on log-sheet. The original data files are `ORFxx.DAT` and `ORFxx.IND` where `xx` is the number in this column.
4. *Sortie*

   Sortie number on log-sheet. In each sortie a new target is measured.
5. *Target*

   Code of target as read from the Recognised Air Picture.
6. *Target no*

   Number of target. For each type of aircraft a unique number is available.
7. *# profs*

   Number of profiles in file. The saturated profiles are excluded. (See chapter 7.)

We have experienced the data transportation from the FELSTAR system to harddisk to be problematic. Downloading a full data buffer to disk took about three hours. Any minor interruption in this process caused the transportation to be aborted and the measured data to be unrecoverably lost. Currently, the FELSTAR is updated to make the data transportation more efficient and robust.

| *Date* | *File* | *Meas.* | *Sor-tie* | *Target* | *Target no* | *# profs* |
|---|---|---|---|---|---|---|
| November 6, 1995 | 0001.mat | 1 | 1 | E120 | 378 | 862 |
| November 13, 1995 | 0002.mat | 7 | 1 | FK10 | 454 | 43 |
| November 13, 1995 | 0003.mat | 8 | 1 | ???? | 1164 | 825 |
| November 14, 1995 | 0004.mat | 11 | 1 | BA46 | 126 | 453 |
| | 0005.mat | | 2 | B73S | 115 | 834 |
| | 0006.mat | | 3 | MD80 | 686 | 706 |
| | 0007.mat | | 4 | FK28 | 457 | 517 |
| | 0008.mat | | 5 | FK10 | 454 | 800 |
| November 14, 1995 | 0009.mat | 12 | 1 | B767 | 121 | 126 |
| | 0010.mat | | 2 | L101 | 628 | 709 |
| | 0011.mat | | 3 | B73S | 115 | 458 |
| November 14, 1995 | 0012.mat | 13 | 1 | B73F | 114 | 623 |
| | 0013.mat | | 2 | B747 | 116 | 743 |
| | 0014.mat | | 3 | FK28 | 457 | 500 |
| | 0015.mat | | 4 | EA31 | 400 | 708 |
| | 0016.mat | | 5 | ???? | 1164 | 365 |
| November 15, 1995 | 0017.mat | 14 | 1 | MD80 | 686 | 209 |
| | 0018.mat | | 2 | B767 | 121 | 907 |
| | 0019.mat | | 3 | FK50 | 458 | 1155 |
| | 0020.mat | | 4 | B73S | 115 | 1202 |
| | 0021.mat | | 5 | EA32 | 401 | 731 |
| | 0022.mat | | 6 | B74F | 117 | 279 |
| November 16, 1995 | 0023.mat | 15 | 1 | SF34 | 964 | 243 |
| | 0024.mat | | 2 | FK10 | 454 | 266 |
| | 0025.mat | | 3 | MD80 | 686 | 247 |
| | 0026.mat | | 4 | B73F | 114 | 115 |
| | 0027.mat | | 5 | B747 | 116 | 1321 |
| | 0028.mat | | 6 | MD80 | 686 | 796 |
| | 0029.mat | | 7 | B767 | 121 | 341 |
| | 0030.mat | | 8 | B73S | 115 | 541 |
| | 0031.mat | | 9 | FK28 | 457 | 25 |
| | 0032.mat | | 10 | FK50 | 458 | 347 |
| | 0033.mat | | 11 | EA31 | 400 | 262 |
| November 20, 1995 | 0034.mat | 17 | 1 | SF34 | 964 | 43 |
| November 22, 1995 | 0035.mat | 18 | 1 | B757 | 120 | 18 |

| *Date* | *File* | *Meas.* | *Sortie* | *Target* | *Target no* | *# profs* |
|---|---|---|---|---|---|---|
| November 22, 1995 | 0036.mat | 19 | 1 | B74F | 117 | 361 |
| | 0037.mat | | 2 | B737 | 113 | 200 |
| | 0038.mat | | 3 | B747 | 116 | 307 |
| | 0039.mat | | 4 | BA46 | 126 | 302 |
| | 0040.mat | | 5 | B73S | 115 | 226 |
| November 28, 1995 | 0041.mat | 20 | 1 | B73S | 115 | 256 |
| | 0042.mat | | 2 | FK10 | 454 | 318 |
| | 0043.mat | | 3 | ???? | 1164 | 48 |
| | 0044.mat | | 4 | B73F | 114 | 230 |
| | 0045.mat | | 5 | ???? | 1164 | 68 |
| | 0046.mat | | 6 | B767 | 121 | 190 |
| | 0047.mat | | 7 | B74F | 117 | 107 |
| November 28, 1995 | 0048.mat | 21 | 1 | B737 | 113 | 190 |
| | 0049.mat | | 2 | FK28 | 457 | 327 |
| November 29, 1995 | 0050.mat | 22 | 1 | L101 | 628 | 133 |
| | 0051.mat | | 2 | B737 | 113 | 230 |
| | 0052.mat | | 3 | B747 | 116 | 438 |
| | 0053.mat | | 4 | E120 | 378 | 215 |
| | 0054.mat | | 5 | B767 | 121 | 401 |
| | 0055.mat | | 6 | B73F | 114 | 158 |
| | 0056.mat | | 7 | SF34 | 964 | 209 |
| | 0057.mat | | 8 | MD80 | 686 | 174 |
| | 0058.mat | | 9 | B74F | 117 | 177 |
| | 0059.mat | | 10 | FK50 | 458 | 354 |
| November 29, 1995 | 0060.mat | 23 | 1 | FK50 | 458 | 358 |
| | 0061.mat | | 2 | FK10 | 454 | 327 |
| | 0062.mat | | 3 | EA31 | 400 | 344 |
| | 0063.mat | | 4 | B73F | 114 | 260 |
| | 0064.mat | | 5 | B737 | 113 | 388 |
| | 0065.mat | | 6 | MD80 | 686 | 357 |
| | 0066.mat | | 7 | E120 | 378 | 502 |
| November 30, 1995 | 0067.mat | 24 | 1 | B737 | 113 | 503 |
| | 0068.mat | | 2 | B767 | 121 | 346 |
| | 0069.mat | | 3 | BA46 | 126 | 544 |
| December 1, 1995 | 0070.mat | 25 | 1 | FK28 | 457 | 212 |
| December 1, 1995 | 0071.mat | 26 | 1 | E120 | 378 | 133 |
| December 1, 1995 | 0072.mat | 27 | 1 | B73F | 114 | 119 |
| | 0073.mat | | 2 | FK50 | 458 | 626 |
| January 5, 1996 | 0074.mat | 28 | 1 | B73S | 115 | 39 |
| January 9, 1996 | 0075.mat | 30 | 1 | MD80 | 686 | 685 |
| | 0076.mat | | 2 | B74F | 117 | 582 |
| | 0077.mat | | 3 | B737 | 113 | 838 |

## 6.2 AWACS interference

The use of a wide-band receiver increases the probability of interference from other transmitters. During the campaign the FELSTAR was used over a wide frequency range, that is 3.07 GHz to 3.52 GHz. Most aircraft were picked up nearby Schiphol so interference with the Air Traffic Control (ATC) radar of Shiphol was unavoidable. For our measurements this appeared not to be a problem, as we would track the aircraft for some time after take-off before the registrations were started. In any way, we did not notice any distortions in our data that could be caused by the Schiphol ATC radars.

A more serious source of interference during the campaign became apparent when a FELSTAR pre-amplifier broke down. After repairing the amplifier and cancelling several obvious reasons for the cause, an extra digital oscilloscope was used to examine whether unexpected signals were present. An unknown interference appeared: the signal came from a search radar and the RF-pulse was frequency modulated. The interference on the sidelobes of the FELSTAR antenna was most of the time too powerful to point the antenna directly at the source of interference. Because of the signal characteristics, the source was soon identified as the *AWACS* (Airborne Warning And Control System). Examining the RAP we soon found this aircraft (which is a Boeing E-3 Sentry). As we suspected that, either directly or indirectly, the AWACS interference caused the break-down of the pre-amplifier, from this moment on all measurements were aborted once the AWACS pulse was detected. Note that the FELSTAR is not designed to withstand jamming or interference from other sources. The power of the AWACS transmissions was far above the normal levels of interference caused by other radars in the vicinity.

Not much later we found out that simply aborting the measurements and saving the data was not enough. During one measurement we saw AWACS pulses on the oscilloscope. The measurements were stopped and the collected data was being downloaded to disk. Normally, the FELSTAR is during this procedure in receive mode. Due to the power of the AWACS pulse (direct) or due to a currently unknown triggering mechanism (indirect) the repaired pre-amplifier broke down again. The remedy was to put the pre-amplifiers in the FELSTAR into the protected mode (T/R switch forced in send mode) when the AWACS pulse was detected.

The AWACS was present during several weeks in November. During these days, only a few short measurements were made.

# 7 Data processing

## 7.1 Definition of coordinate system and aspect angle

For range profiles, important parameters are the aspect azimuth and aspect elevation. Therefore the extraction of these angles from the tracking data needs to be done with great care. In this section we will therefore start with several definitions.

The *target position* as seen from the radar is given in spherical coordinates $(\alpha_r, \theta_r, r)$, see figure 7.1. The azimuth $(\alpha_r)$ is the angle between north and the aircraft direction projected onto the horizontal plane through the radar. The elevation $(\theta_r)$ is the angle between this horizontal plane and the aircraft direction.

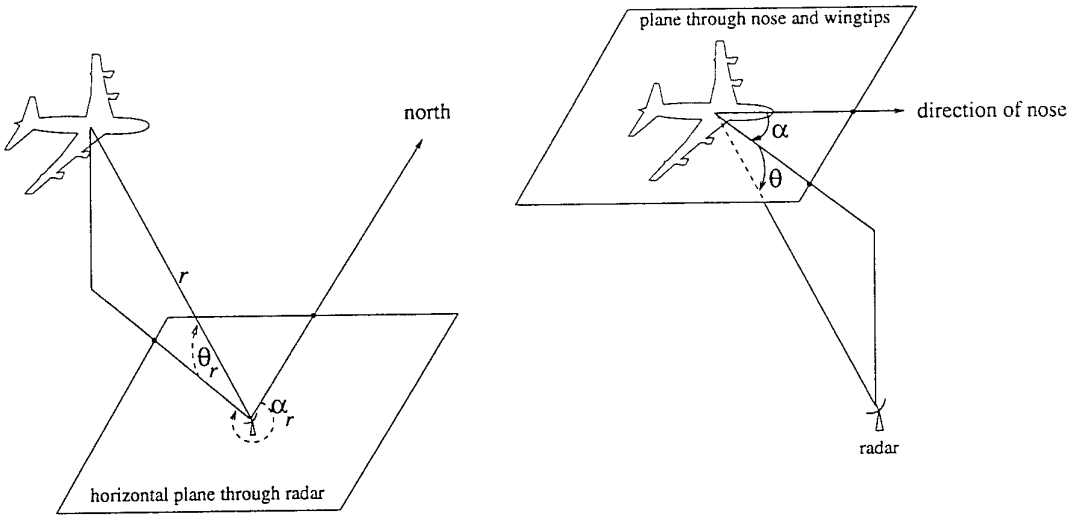


*Figure 7.1*: Definition of the radar coordinate system (left hand side) and the aspect elevation and aspect azimuth (right hand side). In this particular orientation both $\alpha$ and $\theta$ are positive.

The *target aspect angle* can be expressed in a coordinate pair $(\alpha, \theta)$ where $\alpha$ is the *aspect azimuth* and $\theta$ is the *aspect elevation.*

We define the aspect elevation $\theta$ as the angle between the radar line of sight and the plane through the wingtips and nose of the aircraft. The elevation is positive if the aircraft is viewed from underneath. We define the aspect azimuth $\alpha$ as the angle between

- the direction of the nose of the aircraft and
- the direction of the radar line of sight projected on the plane through nose and wingtips.

Note that if the aircraft moves in a horizontal plane, the aspect elevation $\theta$ equals the elevation coordinate $\theta_r$. The aspect azimuth is positive if the aircraft is viewed from the starboard side, it is negative if it is viewed from port side, see figure 7.2.

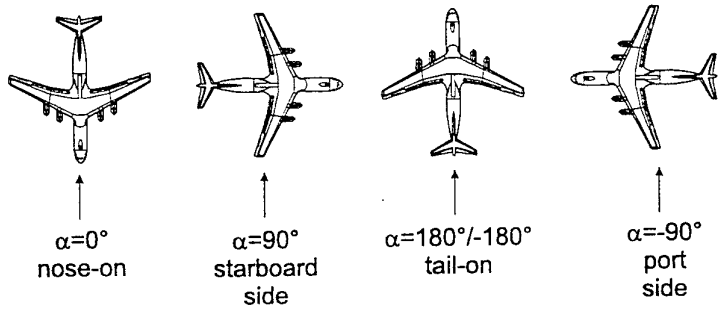


*Figure 7.2*: Aspect azimuth.

To arrive at the elevation angle, the *pitch* angle $\phi$ and the *roll* angle $\rho$ need to be estimated. Figure 7.3 show the definitions of $\phi$ and $\rho$.

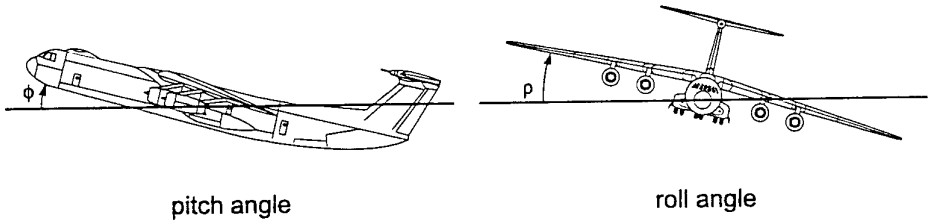


*Figure 7.3*: Roll angle $\rho$ and pitch angle $\phi$.

## 7.2 Selection of signal sample

The pulse has a length of 225 m, the range gate resolution equals 75 m. It means that the aircraft is visible in three of the twenty range cells. The raw data file provides the $(I, Q)$ samples of each of the twenty range-cells per pulse. Also the range $R$ is given: the position of the cell closest to the radar.

The FELSTAR control program was devised such that if one of the target cells comes closer than three samples from the edge of the range gate, the center of the range gate is shifted to the center of the target. The selection of

a single target sample from the twenty samples in a range gate proceeded as follows.

1. Consider all samples that belong to a range profile. We thus have 20 samples/pulse $\times$ 324 pulses = 6480 samples. For each pulse, an azimuth, elevation and range is given.
2. Average the azimuth and elevation over all pulses: this is regarded as *the* azimuth and elevation associated with the range profile.
3. Average the samples of the 324 pulses. Find the position of the maximum over the resulting mean 20 samples. Now select, for each pulse, the $(I, Q)$ values at this position - these are the selected samples. See figure 7.4, left hand side.
4. It occasionally happens that the range gate position is adjusted during the emission of a sweep. The same procedure is then performed twice. See figure 7.4, right hand side.
5. Compute the range from range gate position and the position of the target cell. Do an averaging if the range gate position is adjusted during the emission of a sweep.

## 7.3 Processing of tracking parameters and range profiles

For each batch of subsequently measured range profiles from one target (representing one row in the tables on pages 18 and 19) the following processing sequence was performed. The index $i$ runs over all sweeps within a batch.

1. *Track loss*

   In a few cases during the measurements the track was lost due to a too low signal-to-noise ratio or due to a high saturation. These parts of the data were removed manually.

2. *Tracking parameters*

   For each sweep the time, elevation, azimuth and range is known. We will now describe the extraction of the relevant parameters.

   (a) *Cartesian coordinates*

   Transform the spherical coordinates to cartesian coordinates.

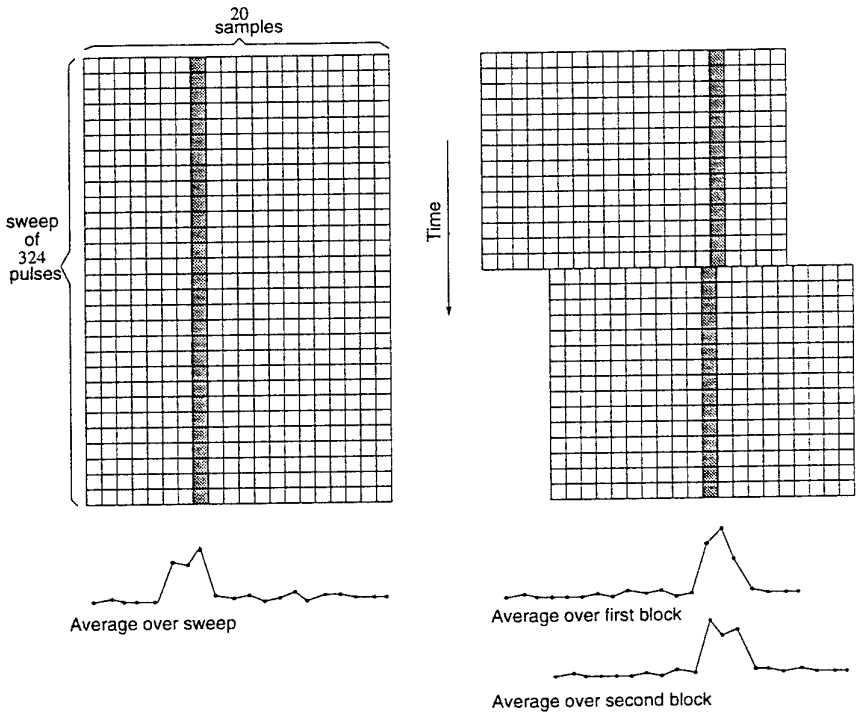


*Figure 7.4*: Signal sample selection for the two possible cases. The gray coloured samples are selected. The figure on the left hand side shows the usual situation: the position of the range gate does not change during the emission of a sweep. The right hand side figure shows the signal selection in case the range gate position changes during the emission of a sweep.

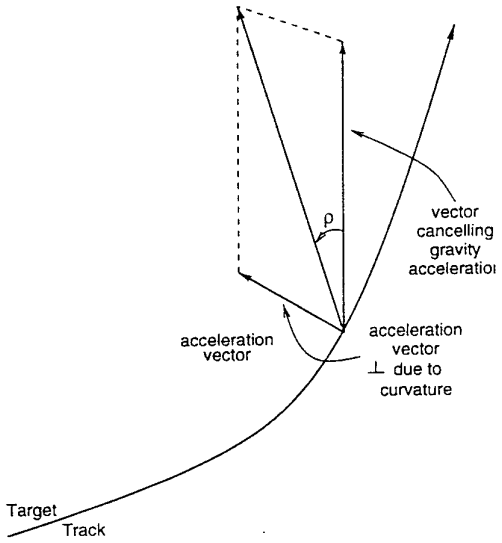


*Figure 7.5*: Estimate of the roll-angle $\rho$. The roll-angle is such that the wings are perpendicular on the acceleration that has to be cancelled by the wings. For this situation, $\rho$ is positive.

(b) *Smoothing*

We used a second order fit over a Gaussian window, width 15 s. That is, we took the coordinate $(x, y, z)_i$ at $t_i$ as a centrepoint, and gave the other target coordinates at $t_j$ the weights $e^{-\frac{1}{2}\frac{(t_i-t_j)^2}{15^2}}$. Then a weighted polynomial of order two is fitted on the set of coordinates of this track. From the polynomial coefficients, the smoothed coordinates $(x_s, y_s, z_s)_i$, the smoothed velocity vector $(v_x, v_y, v_z)_i$ and the smoothed acceleration vector $(a_x, a_y, a_z)_i$ are computed. We repeated this procedure for each $t_i$ where $i$ runs over all sweeps in this batch.

The smoothing is not accurate if a too small number of sweeps is available per measurement (say, less than 50). In those cases, large errors occur in the tracking parameters as the resolution in the range coordinate is only 75 m.

(c) *Roll angle*

We use a simple model to estimate the roll angle $\rho$. We assume that the direction of the acceleration vector that needs to be cancelled by the wings is perpendicular on the wings. This vector has two components: the vector that cancels the gravity and the vector that cancels the curvature acceleration. The latter is the acceleration vector perpendicular on the velocity vector. See also figure 7.5. The roll angle is chosen positive if a left-turn is made,

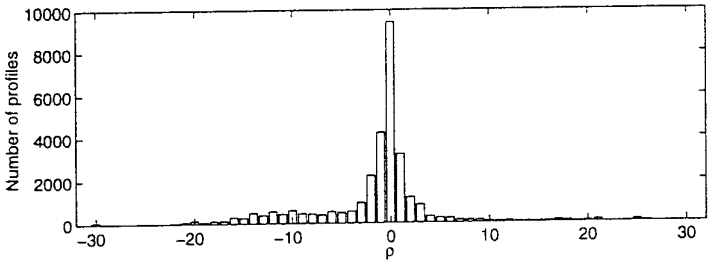


*Figure 7.6*: Histogram of roll angles of all measurements. It shows that more profiles are measured during right-turns then during left-turns.

it is negative if a right-turn is performed. A histogram of all estimated roll angles is shown in figure 7.6.

(d) *Pitch angle*

On first sight, an estimate for the pitch angle $\phi_i$ could be the angle between the horizontal plane and the flight direction:

$$\sin(\phi_i) = \frac{v_{z,i}}{|\vec{v}_i|} \tag{7.1}$$

Although this could be used as a zeroth order estimate for ascending aircraft, it is certainly not appropriate for descending aircraft. In the latter case aircraft always have a *positive* pitch angle whereas the above equation predicts a negative angle. Also, the pitch angle depends on the type of aircraft. Until we have a better model, we will compute the pitch angle according to the above equation, but we will not include it in the computation of the aspect elevation. Figure 7.7 shows a histogram of the pitch angle over all range profiles. It demonstrates that most of the aircraft that we have measured were ascending.

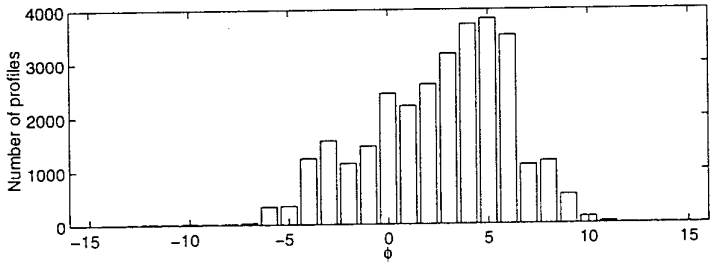


*Figure 7.7*: Histogram of pitch angles of all measurements. It demonstrates that most of the profiles were measured when the targets were gaining height.

(e) *Aspect azimuth*

The aspect azimuth $\alpha_i$ is computed from the angle between the flight direction (from the velocities $v_{x,i}$ and $v_{y,i}$) and the radar line-of-sight (from the smoothed coordinates $x_{s,i}$ and $y_{s,i}$). See figure 7.2.

(f) *Aspect elevation*

If the aircraft flies level in a horizontal plane, the aspect elevation equals the elevation coordinate. We correct this for roll using:

$$\theta_i = \theta_{r,i} + \rho_i \sin(\alpha_i) \tag{7.2}$$

The figure 7.8, 7.9 and 7.10 show for each target (including the unknown targets labelled "????"), the coverage of aspect angle. As the targets are assumed to be symmetrical, the absolute values of the aspect azimuths are shown.

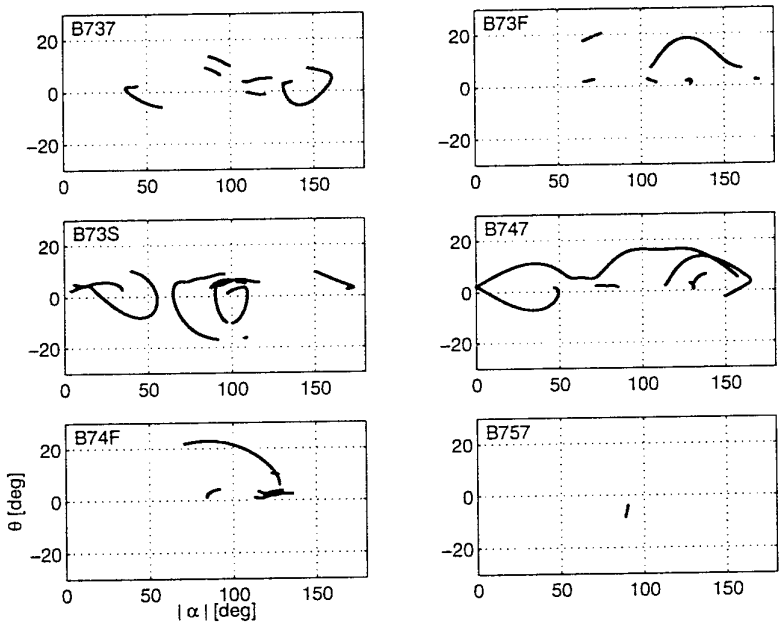


*Figure 7.8*: Aspect angle coverage of targets B737, B73F, B73S, B747, B74F and B757.

(g) *Radial motions*

Finally, the radial accelerations and the radial velocities are computed using the dot-product of the aircraft directions (unity vector) and the aircraft acceleration- and velocity vectors.

Figure 7.11 shows a histogram of the values of the absolute radial accelerations. It shows, as expected, that the accelerations are well below the value where distortions are to be expected.

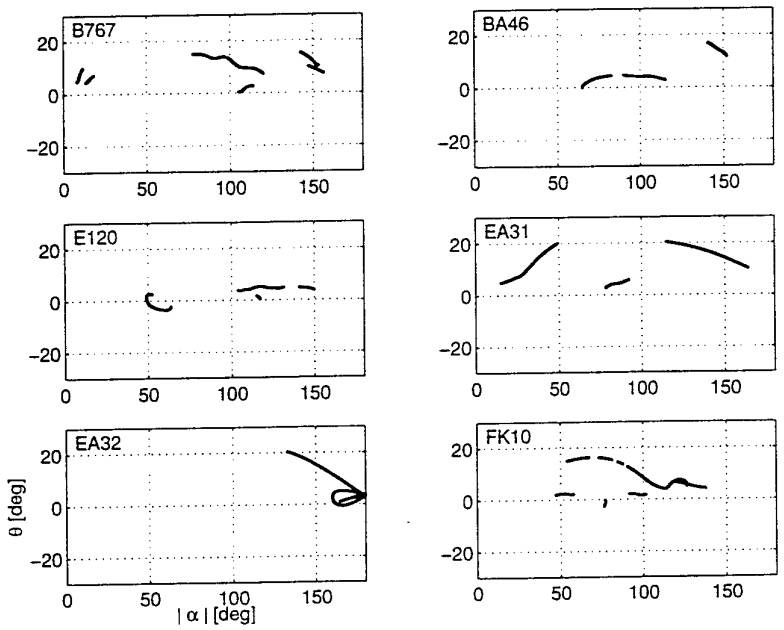


*Figure 7.9*: Aspect angle coverage of targets B767, BA46, E120, EA31, EA32 and FK10.

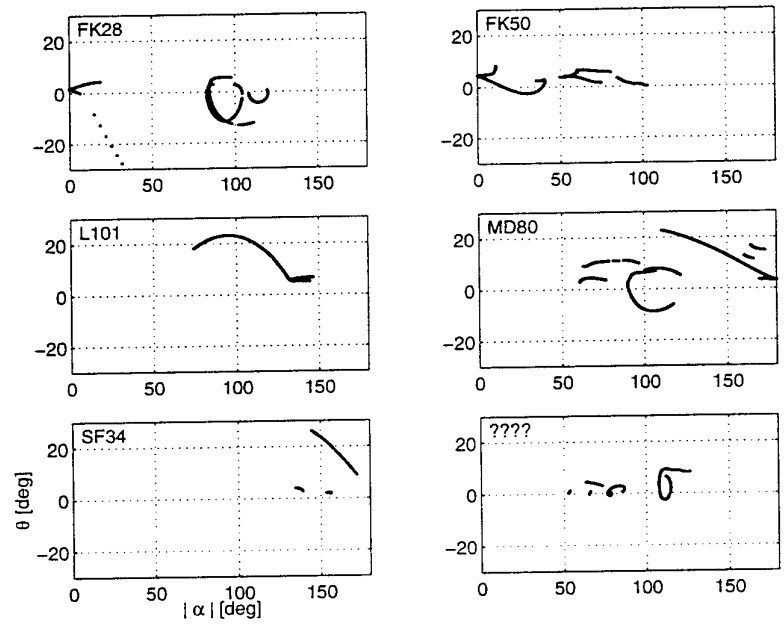


*Figure 7.10*: Aspect angle coverage of targets FK28, FK50, L101, MD80 and SF34. The bottom-right figure shows the aspect angles of the unkown targets.

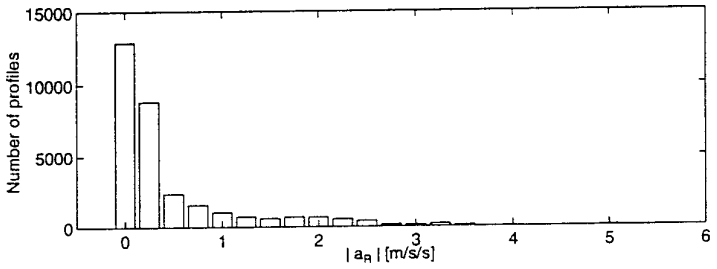


*Figure 7.11*: Histogram of absolute radial accelerations of all measurements

3. *Saturation*

   The FELSTAR has a manual gain control. It occasionally happens that the gain is too high. In this case, *saturation* may occur. It means that either the $I$ or the $Q$ or both have their extreme values of -2048 or 2032. Figure 7.12 shows an example. For each profile a saturation

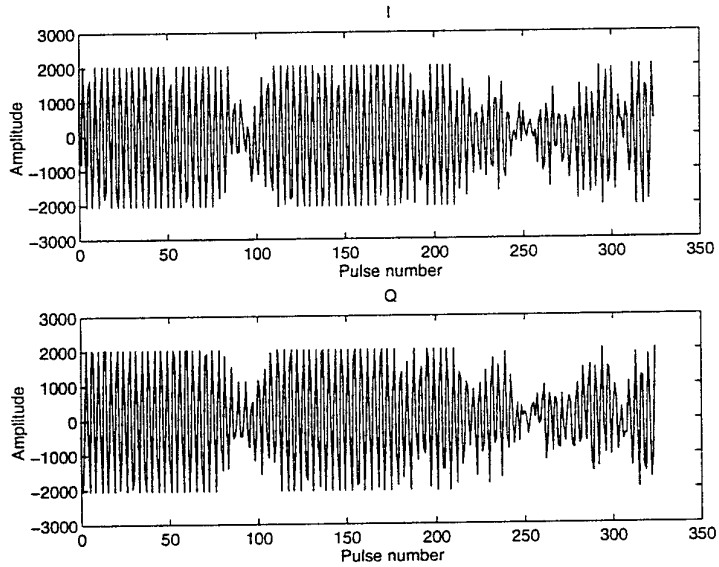


*Figure 7.12*: Samples of a severely saturated sweep. The saturation fraction is 0.53.

   fraction is computed by dividing the number of saturated $(I, Q)$ samples by the total number of samples in the sweep.

   If the saturation fraction is higher than 0.1, we discard the range profile from the measurement.

4. *Calibration*

The following systematical errors may occur in the $(I, Q)$ samples:

(a) *Offset*
Both the $I$ and the $Q$ channel contain a constant offset.

(b) *Imbalance*
The amplification of the $I$ is different from the amplification of $Q$.

(c) *Phase Errors*
The two components $I$ and $Q$ are not perpendicular, so that signal in $I$ leaks to $Q$ and vice versa.

These quantities may vary over the frequency band. The idea is that, averaged over all (non-saturated) sweeps in the ORFEO measurements, the mean of both I and Q should be 0, the fraction of the powers in I and Q should equal unity and the correlation coefficient of I and Q should be zero. Figure 7.13 shows the resulting calibration curves. We used these curves to calibrate the sweeps following the procedure described in reference [5]. The figure shows that for the offset and the imbalance a correction is necessary. The correlation coefficient is systematically non-zero, but the magnitude is small.

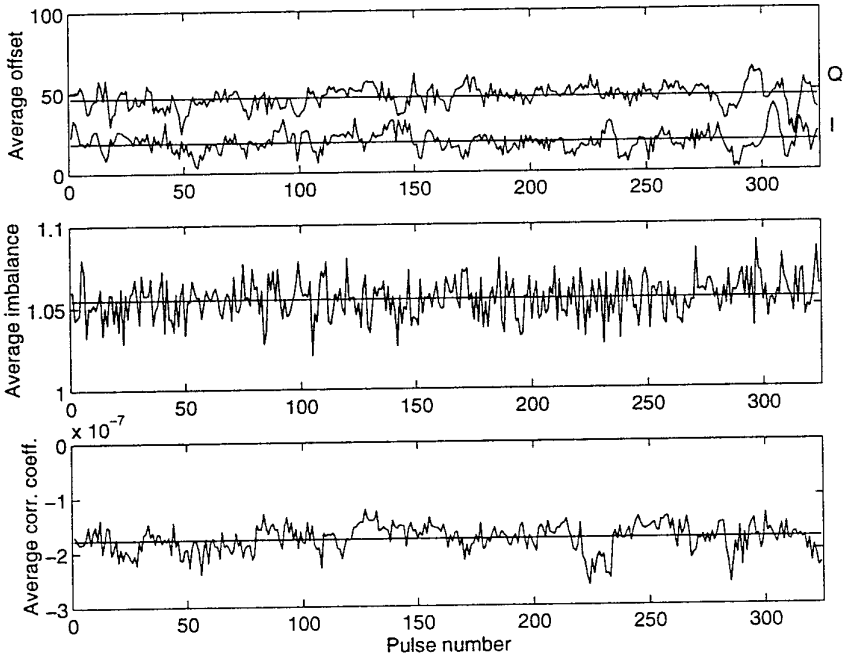


*Figure 7.13*: Calibration curves for the ORFEO measurements.

5. *Transformation to range profiles*

See figure 7.14. After calibration, the range profiles are Hamming weighted, zeropadded to 684 samples, Fourier transformed and squared. The resulting range profile is normalised (such that the total energy equals 1) and centred.

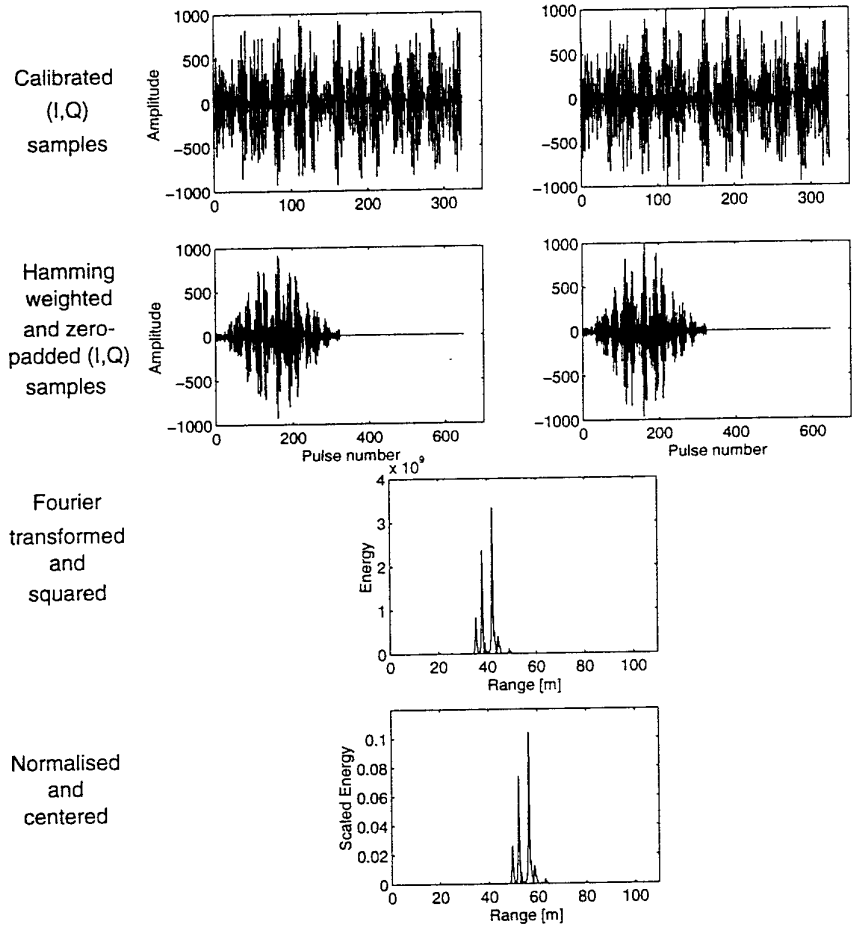


*Figure 7.14*: Transformation of calibrated $(I, Q)$ samples to a range profile. The profile represents the target B73S from file `0020.mat`, viewed at 100° aspect azimuth.

Figure 7.15 shows several examples of radar range profiles of target B73S viewed from different aspect angles.

6. *Signal-to-noise ratio*

   For each profile a signal-to-noise ratio is estimated. The resulting profile has 648 real elements. For the largest aircraft (Boeing 747, $\approx 60$ meters), approximately 425 cells contain the aircraft scatterers. The average energy in a portion of a range profile that is empty is taken as

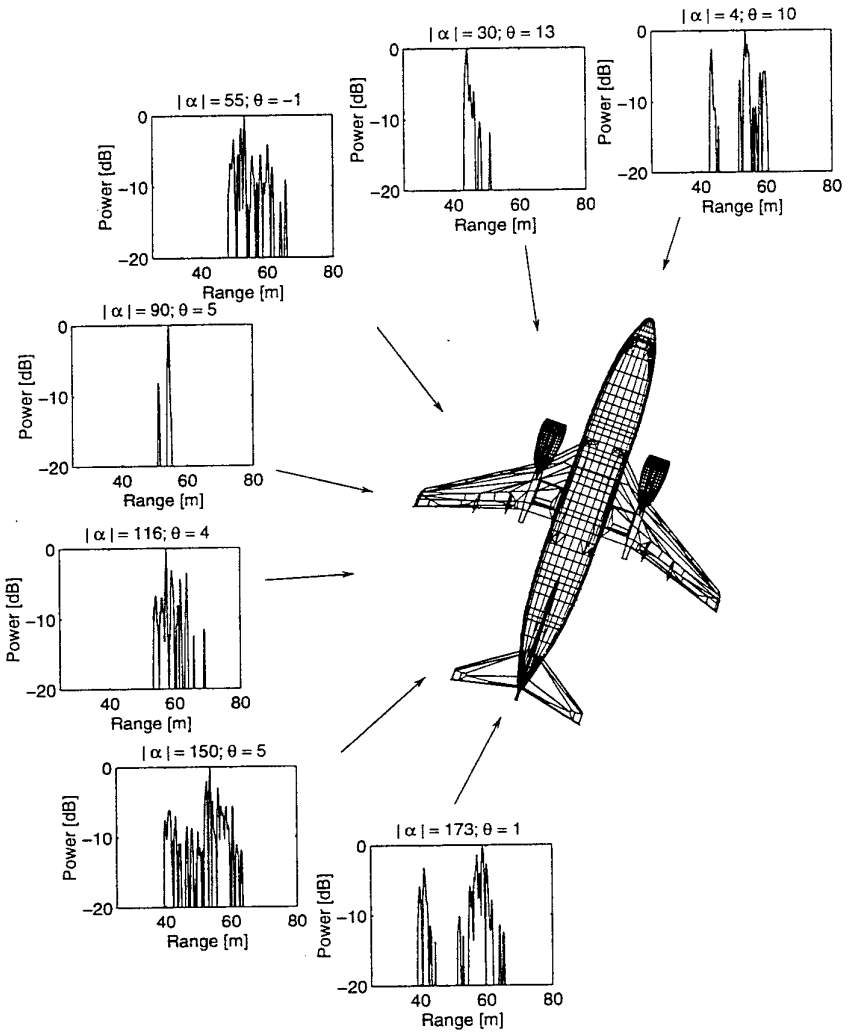


*Figure 7.15*: Range profiles seen under several aspect angles from target B73S. (Geometrical data of Boeing 737-500 from Viewpoint Datalabs.)

the noise on the range profile. First choose the number of cells that is used for noise computation. For our purpose we took ten meters, i.e. 60 range cells. Then make a square window of $324 - 60 = 264$ cells and shift it cyclically over the range profile until the best correlation is found. The cells where the window is zero are averaged to find the $E_{\text{empty}}$, the energy in the empty cells. This is an estimate of the noise in the range profile.

Now let us find the cells for the computation of the signal. The smallest aircraft has a size of approximately 20 meters. Let us assume that, in the worst case due to obscuration, this aircraft is visible over 5 meters. This corresponds to 30 range cells. Let a rectangular window with a size of 30 range cells slide over the range profile. At the best match, the cell-contents are averaged to find $E_{\text{filled}}$. This is an estimate of the signal *plus* noise. See also figure 7.16.

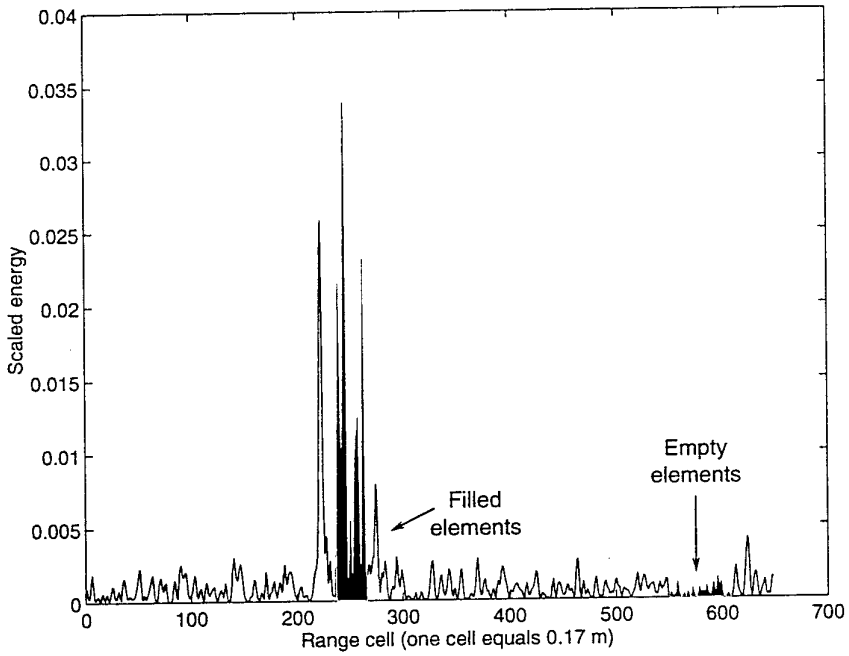


*Figure 7.16*: Estimate of signal-to-noise ratio. The surfaces under the curves used for the computation of the signal to noise ratio are coloured black. For this profile (file `0001.mat`, target `E120`) the signal to noise ratio was estimated to be 13.8 dB.

The signal to noise ratio $SNR$ is now estimated by

$$< SNR >= 10 \log_{10}(\frac{E_{\text{filled}}}{E_{\text{empty}}} - 1) \tag{7.3}$$

We are aware that this measure of the signal-to-noise ratio is an *overestimate* because it relates to the best visible part of the aircraft.

. Figure 7.17 shows a histogram of the signal-to-noise ratios for all range profiles.

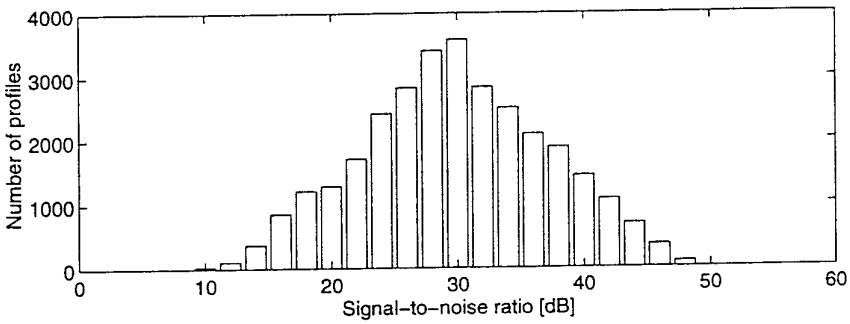


*Figure 7.17*: Histogram of signal-to-noise ratios of all ORFEO range profiles.

# 8 Concluding remarks

In this report we have described the ORFEO measurement campaign.

1. The acquisition of an NCTR database using the FELSTAR in combination with the Recognised Air Picture has shown to be very fruitful.
2. For the first time, we have used the Velocity Tolerant Waveform for measuring radar range profiles. It proved to be successful: motion compensation was not necessary and no range profile distortion due to JEM lines was observed.
3. We have described and performed several processing steps, such as the estimate of tracking parameters and orientation of the aircraft, removal of saturated range profiles and estimates of signal-to-noise ratios. Calibration, i.e. removing systematic errors from the raw samples, has shown to be an essential part of the processing.
4. If we consider the coverage of aspect angle, the ORFEO database alone is *not* large enough for building a range profile classification system for the FELSTAR. We therefore recommend to improve the data transportation from the FELSTAR to harddisk and, once this has been done, to perform more measurements.
5. Despite the problems with the data transportation and the AWACS interference, the database is judged to be large enough for a first comparison between FELSTAR range profiles and profiles that are computed using RCS-prediction techniques.

# 9 References

[1] M.G.E. Brand.
Radar signature analysis and prediction by physical optics and ray tracing. The RAPPORT code for RCS prediction.
FEL-95-A097, TNO-FEL, 1995.

[2] E.C. Burt, T.G. Moore, and B.W. Zuerndorfer.
Enhanced resolution imagery from limited data.
In *Workshop on "Radar Imaging and Classification Techniques", AC/243 (Panel 10) RSG.12 TP/1*, February 1993.

[3] R. van der Heiden.
Waveforms for range profile generation - application on the FELSTAR radar.
FEL-93-A068, TNO-FEL, 1994.

[4] R.G. Aldous.
Private communication.

[5] R. van der Heiden and Ph. van Dorp.
Calibration and format of the FELSTAR/AIDA data.
Annex to the EXABYTE data tape released for AC/243 (Panel 10/RSG12), December 1993.

# 10 Signature

H.R. van Es
Group leader

R. van der Heiden
Project leader/Author

# REPORT DOCUMENTATION PAGE
## (MOD-NL)

| 1. DEFENCE REPORT NO (MOD-NL) | 2. RECIPIENT'S ACCESSION NO | 3. PERFORMING ORGANIZATION REPORT NO |
|---|---|---|
| TD96-0074 | | FEL-96-A073 |
| **4. PROJECT/TASK/WORK UNIT NO** | **5. CONTRACT NO** | **6. REPORT DATE** |
| 24357 | A94KM673 | August 1996 |
| **7. NUMBER OF PAGES** | **8. NUMBER OF REFERENCES** | **9. TYPE OF REPORT AND DATES COVERED** |
| 37 (excl RDP & distribution list) | 5 | |

**10. TITLE AND SUBTITLE**

The ORFEO measurement campaign

**11. AUTHOR(S)**

R. van der Heiden, J. de Vries

**12. PERFORMING ORGANIZATION NAME(S) AND ADDRESS(ES)**

TNO Physics and Electronics Laboratory, PO Box 96864, 2509 JG The Hague, The Netherlands
Oude Waalsdorperweg 63, The Hague, The Netherlands

**13. SPONSORING AGENCY NAME(S) AND ADDRESS(ES)**

DMKM/WCS/COSPON
Van der Burchlaan 31, 2597 PC The Hague, The Netherlands

**14. SUPPLEMENTARY NOTES**

The classification designation Ongerubriceerd is equivalent to Unclassified, Stg. Confidentieel is equivalent to Confidential and Stg. Geheim is equivalent to Secret.

**15. ABSTRACT (MAXIMUM 200 WORDS (1044 BYTE))**

During the fall of 1995 at TNO-FEL the ORFEO measurement campaign was held using the FELSTAR S-band radar. The objective was to acquire a database of radar range profiles of civil aircraft. This report describes the measurement procedures, the instrumentation, the waveform choice, the signal processing and the results of the campaign. ORFEO was successful: over 30,000 range profiles from 17 different aircraft were measured.

| 16. DESCRIPTORS | IDENTIFIERS |
|---|---|
| Target Recognition<br>Radar<br>High Resolution Radar<br>Signal Processing<br>Surveys | Radar Range Profiles<br>Non-cooperative Target Recognition |

| 17a. SECURITY CLASSIFICATION (OF REPORT) | 17b. SECURITY CLASSIFICATION (OF PAGE) | 17c. SECURITY CLASSIFICATION (OF ABSTRACT) |
|---|---|---|
| Ongerubriceerd | Ongerubriceerd | Ongerubriceerd |

| 18. DISTRIBUTION AVAILABILITY STATEMENT | 17d. SECURITY CLASSIFICATION (OF TITLES) |
|---|---|
| Unlimited Distribution | Ongerubriceerd |

# Distributielijst

| | |
|---|---|
| 1. | Bureau TNO Defensieonderzoek |
| 2. | Directeur Wetenschappelijk Onderzoek en Ontwikkeling*) |
| 3. | HWO-KL*) |
| 4. | HWO-KLu*) |
| 5. | HWO-KM |
| 6. | HWO-CO*) |
| 7 t/m 9. | KMA, Bibliotheek |
| 10. | DMKM/WCS/COSPON, t.a.v. Drs. W. Pelt |
| 11. | KIM, t.a.v. Ir. B. Bruggeman |
| 12. | DMKL/Beleid, t.a.v. Ir. N. Pos |
| 13. | DMKM/WCS/EMDC*) |
| 14. | ANCP 1.30, t.a.v. Dr. P.N.R. Stoyle, Defence Research Agency |
| 15. | Directie TNO-FEL, t.a.v. Dr. J.W. Maas |
| 16. | Directie TNO-FEL, t.a.v. Ir. J.A. Vogel, daarna reserve |
| 17. | Archief TNO-FEL, in bruikleen aan M&P*) |
| 18. | Archief TNO-FEL, in bruikleen aan Ir. C. Eberwijn |
| 19. | Archief TNO-FEL, in bruikleen aan Ir. G.A. van der Spek |
| 20. | Archief TNO-FEL, in bruikleen aan Ir. H.R. van Es |
| 21. | Archief TNO-FEL, in bruikleen aan Ir. A.G. Huizing |
| 22. | Archief TNO-FEL, in bruikleen aan Drs. R. van der Heiden |
| 23. | Archief TNO-FEL, in bruikleen aan J. de Vries |
| 24. | Documentatie TNO-FEL |
| 25 t/m 29. | Reserve |
| | TNO-PML, Bibliotheek**) |
| | TNO-TM, Bibliotheek**) |
| | TNO-FEL, Bibliotheek**) |

Indien binnen de krijgsmacht extra exemplaren van dit rapport worden gewenst door personen of instanties die niet op de verzendlijst voorkomen, dan dienen deze aangevraagd te worden bij het betreffende Hoofd Wetenschappelijk Onderzoek of, indien het een K-opdracht betreft, bij de Directeur Wetenschappelijk Onderzoek en Ontwikkeling.

*) Beperkt rapport (titelblad, managementuittreksel, RDP en distributielijst).
**) RDP.